Photoemission and the Electronic Structure of $PuCoGa_5$

J. J. Joyce,* J. M. Wills, T. Durakiewicz, M. T. Butterfield, E. Guziewicz, J. L. Sarrao, L. A. Morales, and A. J. Arko
Los Alamos National Laboratory, Los Alamos, New Mexico 87545, USA

O. Eriksson
Department of Physics, Uppsala University, Box 530, Uppsala, Sweden
(Received 3 June 2003; published 22 October 2003)

The electronic structure of the first Pu-based superconductor $PuCoGa_5$ is explored using photoelectron spectroscopy and a novel theoretical scheme. Exceptional agreement between calculation and experiment defines a path forward for understanding the electronic structure aspects of Pu-based materials. The photoemission results show two separate regions of $5f$ electron spectral intensity, one at the Fermi energy and another centered 1.2 eV below the Fermi level. The results for $PuCoGa_5$ clearly indicate $5f$ electron behavior on the threshold between localized and itinerant. Comparisons to delta phase Pu metal show a broader framework for understanding the fundamental electronic properties of the Pu $5f$ levels in general within two configurations, one localized and one itinerant.

DOI: 10.1103/PhysRevLett.91.176401 PACS numbers: 71.27.+a, 71.28.+d, 79.60.–i

The recent discovery of $PuCoGa_5$, the first Pu-based superconductor, with a $T_C = 18.5$ K and unconventional superconductivity demonstrates the rich and complex nature of Pu-based materials [1]. The role of the $5f$ electrons in bonding and hybridization is intimately intertwined with the wide range of ground state properties found in actinide materials including enhanced mass, magnetism, superconductivity, as well as spin and charge density waves. Within the actinide series, Pu occupies the position between the clearly hybridized $5f$ states of uranium [2] and clearly localized $5f$ states of americium [3] which due to its $J = 0$ ground state is a superconductor. Pu defines the localized-itinerant boundary for the $5f$ electrons in the actinides [4,5]. There have been several recent papers reporting photoemission [6–9] and electronic structure calculations [4,5,10–14] for the fcc (δ) phase of Pu metal. A classic failure of density functional theory (DFT) within the local density approximation (LDA) or generalized gradient approximation (GGA) is observed in the case of δ-Pu with the volume from LDA falling over 25% short (GGA only slightly better) of the experimental volume in the largest discrepancy to date in DFT for a crystal.

To accommodate the large volume of the delta phase of Pu metal, there have been magnetically ordered electronic structures proposed which, to some degree, effectively localize $5f$ electrons, reducing the contribution to the chemical bonding and increasing the volume [10]; however, there is no experimental evidence for magnetism in δ-Pu [15]. Another approach used for δ-Pu is the dynamical mean field theory (DMFT) which may offer promise with further development [11]. Currently the agreement between DMFT and experiment is weak with the photoelectron spectroscopy (PES) shown in Ref. [11] being more of an idealized representation than actual data. The link between δ-Pu metal and $PuCoGa_5$ is strong and follows the same path as the family of Ce-based heavy fermion superconductors ($CeMIn_5$, $M = $ Co, Rh, Ir) [16] having the cubic $CeIn_3$ as the root crystal structure. Here we have δ-Pu as the parent cubic phase structure with Ga substituting on the face centers to form $PuGa_3$ and insertion of the $CoGa_2$ layer into the cubic structure to form $PuCoGa_5$ in the tetragonal phase. With the discovery of superconductivity in $PuRhGa_5$ [17] it does indeed seem reasonable that the $PuMGa_5$ family of compounds is following systematics much like the $CeMIn_5$ family of superconducting compounds.

Since the discovery of $PuCoGa_5$ there are currently three computational frameworks to describe the electronic structure of $PuCoGa_5$ nominally within the framework of DFT [18–20]. The theoretical efforts for $PuCoGa_5$ are following the path set forth in δ-Pu, with conventional DFT pushing the $5f$-electron intensity up against the Fermi level [18] or magnetic solutions [19] which serve to effectively localize some of the Pu $5f$ intensity below the Fermi level (E_F). For $PuCoGa_5$, as in δ-Pu, there is no experimental evidence for ordered magnetism. However, the magnetic solutions for both δ-Pu and $PuCoGa_5$ provide valuable insight into the electronic structure. The agreement between PES and calculation is improved in the magnetic calculations compared with conventional DFT calculations without magnetism. The magnetic state, which to some extent, effectively localizes f electrons and removes them from the Fermi energy provides the needed spectral intensity away from the Fermi level to match the PES results [10,19].

Understanding the nature of the $5f$ electrons is central to understanding the electronic properties of $PuCoGa_5$ as well as the broader Pu electronic structure problem. There is little photoemission data on metallic Pu systems beyond Pu itself with data for PuSe and PuSb appearing recently [21]. In this Letter we present experimental evidence for the Pu $5f$ electrons in two configurations, one well removed from E_F and one directly at E_F in a

peak consistent with narrow band characteristics of other actinides [22]. Additionally, a mixed-level model (MLM) calculation is presented showing remarkable agreement with the PES data where the Pu $5f$ electrons exist in two configurations, one localized and one itinerant [6,13,14]. The agreement between the model calculation and the PES data surpasses that found for the MLM and PES in δ-Pu [6,14] which was already qualitatively the best agreement between calculation and PES (while preserving the known nonmagnetic ground state).

Single crystals of multimillimeter dimension $PuCoGa_5$ were grown by the flux growth method. The PES samples were from the same flux growth batch as samples described in the discovery paper which documents characterization [1]. The resistivity just above T_C and the reproducibility of T_C between single crystals [1] and polycrystals [17] indicate the high quality and robustness of the sample stoichiometry. Rectangular samples were selected for mounting and ordered along a low symmetry crystallographic direction. The analyzer acceptance angle was $\pm 8°$ thus covering the reciprocal lattice at $h\nu = 40.8$ eV and the data collection geometry was perpendicular to the sample surface. The sample surface was cleaned by laser ablation at a temperature (T) of 77 K in a vacuum of 6×10^{11} Torr. Laser ablation has been shown to be an excellent choice of surface preparation for actinides [6,7]. There were no spectroscopic features identifiable as surface related in the staged cleaning of the sample surface from native oxide through clean metallic surface. There was no sample surface contamination in the spectra with the 40.8 eV data having a sensitivity of about 5% of a monolayer for oxide-related degradation [6,8]. The UV light source utilizes the He_I (21.2 eV), $He_{II\alpha}$ (40.8 eV), and $He_{II\beta}$ (48.4 eV) lines. The energy resolution of the instrument (ΔE) was 60–120 meV with $T = 77$ K and $PuCoGa_5$ in the normal state. With the three photon energies ($h\nu$) one may obtain a qualitative assessment of the orbital sections for the major electronic levels, Pu $5f$, Pu $6d$, and Co $3d$. The remaining levels (Ga $4s, 4p$, Co $4s$, Pu $7s$) show smaller cross sections over this energy range. Using the atomic cross sections from Yeh and Lindau [23] as a qualitative guide one sees the Pu $5f$ and the Co $3d$ levels increasing from 21.2 through 48.4 eV while the Pu $6d$ level is decreasing. At $h\nu = 40.8$ eV the cross section per electron for the Pu $5f, 6d$ and Co $3d$ levels are comparable and so this is a favorable energy to compare against calculation. The assumption of a comparable cross section at 40.8 eV has been explored for δ-Pu where the transition matrix elements were calculated at 40.8 eV and compared with the density of states showing only minor variations [14]. In addition to the matrix element calculations, the agreement between PES and MLM for δ-Pu in Ref. [14], and here for $PuCoGa_5$, gives strong support for considering the PES spectra as representative of the electronic structure and not influenced in a substantive way by final state, satellite, or screening effects not already accounted for in the model or processing of the data.

The basis of the MLM is a partitioning of the electron density into localized and delocalized parts, minimizing the total energy (including a correlation energy associated with localization) with respect to the partitioning [14]. The total energy of $PuCoGa_5$, and of δ-Pu, becomes minimized for an atomic $5f^4$ configuration with roughly one $5f$ electron in a delocalized Bloch state. The four localized $5f$ electrons couple into a singlet, a many-body effect that is not accounted for within a single-particle picture. The hybridization between the conduction band states and the localized f states (here a four electron multiplet state) is a key interaction needed to produce an accurate theoretical spectrum placing the MLM beyond the capacity of single-particle models such as LDA and GGA. The hybridization matrix element is calculated from the width of the $5f$ resonance which is proportional to the $5f$ electron wave function at the muffin-tin sphere. Our value is consistent with the fact that spin and orbital couplings within the $5f$ shell are important in this system. In addition to a broadening of the $5f$ level, the hybridization matrix elements cause a reduction in the spectral weight. Hence the hybridization results in a broadening and a shift of the spectral weight.

In Fig. 1 we present the first photoemission data on $PuCoGa_5$. The spectrum was acquired at $T = 77$ K, $\Delta E = 75$ meV, and $h\nu = 40.8$ eV. The valence band spectrum

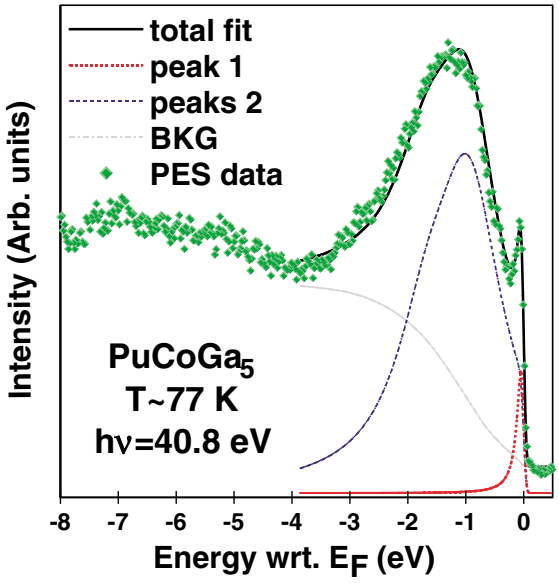

FIG. 1 (color online). The photoemission spectrum for $PuCoGa_5$ at $h\nu = 40.8$ eV and $T = 77$ K is shown with $\Delta E = 75$ meV. The data show a narrow feature at E_F, a broad manifold 1.2 eV lower, and two smaller features at 5 and 7 eV below E_F. Also shown is the line shape analysis with a narrow peak cut by the Fermi function, and a broad feature centered on 1.2 eV made up of two components (diamonds: data, solid line: total fit, dotted line: Fermi level peak, dashed line: main peak, and dot-dashed line: background).

in Fig. 1 contains three regions of interest: a sharp peak at E_F, a broad manifold centered 1.2 eV below E_F, and two small features at 5 and 7 eV below E_F, which most likely arise from the Ga and Co sp electrons. Along with the data we show line shape analysis for the first 4 eV of the valence band. We use a Gaussian function for ΔE, a Lorentzian for the photohole lifetime (natural linewidth), and a 77 K Fermi function. The fitting shows two distinct regions in the valence band, a narrow peak at E_F with a width on the occupied side of E_F of 100 meV, and a broad manifold centered at -1.2 eV which is composed of two smaller peaks at -1 and -1.75 eV below E_F. The narrow peak near E_F is directly cut by the Fermi function. The narrow peak at E_F is very similar to such features found in several U compounds exhibiting narrow band behavior [22]. The fit to the data is good and the general description is consistent with that of δ-Pu [6,8] showing two main regions of spectral intensity, both with substantial $5f$ contributions. In the case of $PuCoGa_5$ shown in Fig. 1 the main intensity around -1.2 eV is a superposition between Pu $5f$ and Co $3d$ states.

The PES data and two theoretical calculations are shown in Fig. 2. For cross-section reasons detailed above, the PES data were taken at $h\nu = 40.8$ eV and compared to the calculations. The PES data are shown as diamonds, a GGA calculation as a dot-dashed line, and a calculation based on the mixed-level model shown as a dashed line. As in the line shape analysis in Fig. 1, these calculations were Gaussian broadened for ΔE, Lorentzian broadened for photohole lifetime (with E^2 dependence consistent

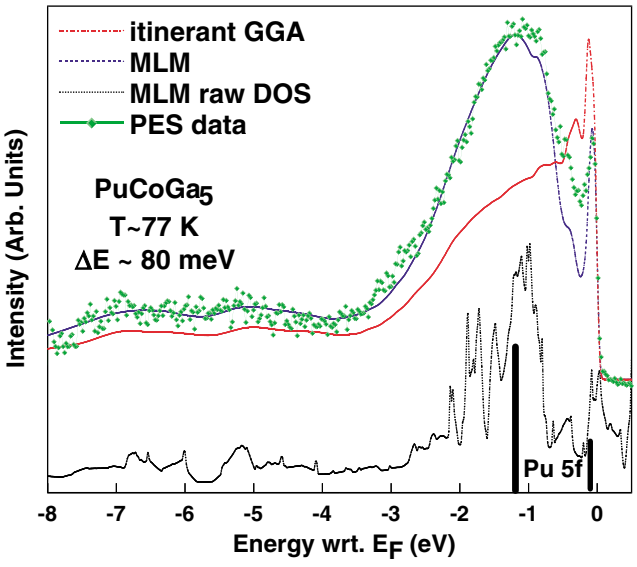

FIG. 2 (color online). The photoemission data for $PuCoGa_5$ is compared against model calculations. The experimental valance band PES data is shown as diamonds, a GGA calculation as a dot-dashed line, a MLM calculation as a dashed line, and a raw MLM DOS as a dotted line (f-electron postion centers are represented by solid bars). The calculations (less the raw DOS) have been processed for photohole lifetime, instrument, and Fermi function broadening.

with Fermi liquid theory), and the appropriate Fermi function for temperature. The above broadenings are not adjustable fitting parameters but rather fixed by known values of temperature, resolution, and model lifetime. The dotted line is the MLM calculation without the broadenings. The bars are the nominal starting values for Pu $5f$ electron positions, the large bar for the localized manifold, and the small bar the one $5f$ electron fully participating in the bonding. This delocalized $5f$ electron is part of the band structure calculation and fully hybridized with the conduction electrons with $5f$ character spread over an energy range of more than 1 eV. The PES data indicate that some significant fraction of this delocalized $5f$ weight resides with the E_F peak. First, we note that the GGA calculation does not show particularly good agreement with the PES data, presenting the shortcomings for a GGA calculation with an open f shell which concentrates the f weight at E_F (similar to the calculations of Ref. [18]). However, the mixed-level model calculation shows remarkable agreement with the PES data. The calculation matches the data over the entire valence band region from the peak at the Fermi level through the main broad manifold at -1.2 eV to the two smaller features at 5 and 7 eV related to the sp electrons. Even the small shoulder in the PES data at -0.5 eV is reproduced in the calculation.

This level of agreement would be very good between PES data and a calculation for a simple metal or semiconductor; for a complex, ternary, Pu-based material it is exceptional. In particular, the peak at the Fermi level shows not only the correct energy and width, it also shows the correct ratio of spectral intensity to the main emission peak at -1.2 eV as well as the smaller features at 5 and 7 eV. The ratio of spectral intensities is important within the MLM framework in order to validate against experiment the fraction of localized vs itinerant electrons in the calculation. In our calculations the total energy is minimized when four out of five $5f$ electrons are localized. Within the MLM computational framework, this represents a minimum in total energy compared with any other configuration (0, 1, 2, 3, or 5 Pu $5f$ electrons localized). This configuration also results in the correct volume for the unit cell, compared with the experimental lattice constant. This same solution was found for δ-Pu [13,14] (see Fig. 2 of Ref.[13]) and the plot of total energy vs volume is very similar for δ-Pu and $PuCoGa_5$. The notion of the $5f$ electrons in Pu occurring in two different configurations for δ-Pu metal, one localized and one hybridized, was initially put forward independently on the experimental [7] and computational [13] fronts. With the results shown in Fig. 2 it would seem reasonable that this model for δ-Pu also works well for $PuCoGa_5$ and may have broad applications for Pu-based materials in general.

In Fig. 3 we show the valence band PES data for $PuCoGa_5$ as a function of photon energy at 21.2, 40.8, and 48.4 eV. The main valence band feature (-1.2 eV) does not change width or shape substantially over this

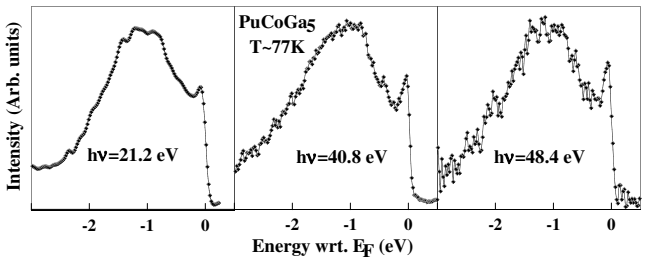

FIG. 3. Photoemission data taken with photon energies of 21.2, 40.8, and 48.4 eV. There is an increase in intensity of the peak at E_F with respect to the main spectral intensity at 1.2 eV consistent with the peak at E_F containing substantial but not exclusive Pu $5f$ character, while the main peak centered at -1.2 eV is characterized by Pu $5f$ as well as Co $3d$ intensity.

photon energy range. The peak at E_F grows with respect to the main peak centered at -1.2 eV. The growth in intensity of the peak at E_F combined with the narrowness of this spectral feature gives a strong indication that this peak contains substantial $5f$ electron character. The itinerant nature of the peak cut by the Fermi energy is not in question, but the extent of hybridization with conduction electrons is difficult to quantify. The existence of the peak at 21.2 eV, although small, probably indicates some non-f-electron character to the spectral feature. A narrow itinerant peak with substantial $5f$ character at the Fermi level is also consistent with the MLM calculation for $PuCoGa_5$.

The main peak in the PES spectrum at -1.2 eV is most likely a superposition of Pu $5f$ and Co $3d$ states. Both the Co $3d$ and Pu $5f$ cross sections are increasing as a function of photon energy over the 21 to 41 eV interval, the Pu $5f$ cross section increases by roughly a factor of 6, while the Co $3d$ cross section doubles in value [23]. These differences account for the increase in the E_F peak over the main peak since the E_F peak contains primarily $5f$ character and the main peak a mix of $3d$ and $5f$ character. Also, the $5f$ character of the main peak would be necessitated by the relative intensities of the main peak and the Fermi level peak at 40.8 and 48.4 eV since a vast majority (over 90%) of the spectral weight is in the main peak it would be inconsistent to consider all of the $5f$ electrons in Pu to reside in the E_F peak and the main peak to consist exclusively of Co $3d$ states. The composition of the main peak being a mixture of Co $3d$ and localized Pu $5f$ electrons is consistent with the MLM calculation for $PuCoGa_5$ which shows the strongest Co $3d$ intensity in the energy interval -0.75 to -2 eV.

In summary, the PES data for $PuCoGa_5$ give a solid indication of the Pu $5f$ electrons occurring in two configurations, one itinerant and being located at the Fermi level, the other localized and centered 1.2 eV below E_F. The MLM calculation shows this same Pu $5f$ arrangement, with one $5f$ electron being itinerant and the other four $5f$ electrons being localized. The agreement between PES and the MLM for $PuCoGa_5$ is impressive. This electronic structure arrangement with the $5f$ electrons in a dual mode is also found in δ-Pu metal [6,14]. With reliable PES data that are in good agreement with theoretical calculations, which also give good volumes and the correct magnetic configuration, a path forward for understanding the complex electronic structure of Pu-based materials is at hand.

This work was performed under the auspices of the U.S. Department of Energy, Office of Science and LANL LDRD program.

*Electronic address: jjoyce@lanl.gov

[1] J. L. Sarrao *et al.*, Nature (London) **420**, 297 (2002).
[2] H. G. Smith *et al.*, Phys. Rev. Lett. **44**, 1612 (1980); Lars Fast *et al.*, Phys. Rev. Lett. **81**, 2978 (1998).
[3] J. L. Smith and R. G. Haire, Science **200**, 535 (1978); B. Johansson and A. Rosengren, Phys. Rev. B **11**, 2836 (1975).
[4] M. S. S. Brooks, H. L. Skriver, and B. Johansson, in *Handbook on the Physics and Chemistry of the Actinides*, edited by A. J. Freeman and G. H. Landers (North-Holland, Amsterdam, 1984).
[5] I. V. Solovyev *et al.*, Phys. Rev. B **43**, 14 414 (1991).
[6] A. J. Arko *et al.*, Phys. Rev. B **62**, 1773 (2000).
[7] J. J. Joyce *et al.*, Surf. Interface Anal. **26**, 121 (1998).
[8] L. Havela *et al.*, Phys. Rev. B **65**, 235118 (2002); T. Gouder *et al.*, Europhys. Lett. **55**, 705 (2001); T. Almeida *et al.*, Surf. Sci. **287**, 141 (1993).
[9] J. Terry *et al.*, Surf. Sci. **499**, L141 (2002).
[10] Per Soderlind, Alex Landa, and Babak Sadigh, Phys. Rev. B **66**, 205109 (2002).
[11] S. Y. Savrasov, G. Kotliar, and E. Abrahams, Nature (London) **410**, 793 (2001).
[12] J. Bouchet *et al.*, J. Phys. Condens. Matter **12**, 1723 (2000).
[13] O. Eriksson *et al.*, J. Alloys Compd. **287**, 1 (1999).
[14] J. M. Wills *et al.*, cond-mat/0307767.
[15] See articles in *Handbook on the Physics and Chemistry of the Actinides*, edited by A. J. Freeman and G. H. Landers (North-Holland, Amsterdam, 1984).
[16] H . Hegger *et al.*, Phys. Rev. Lett. **84**, 4986 (2000); C. Petrovic *et al.*, Europhys. Lett. **53**, 354 (2001); C. Petrovic *et al.*, J. Phys. Condens. Matter **13**, L337 (2001).
[17] F. Wastin *et al.*, J. Phys. Chem. (to be published).
[18] A. Szajek and J.A. Morkowski, J. Phys. Condens. Matter **15**, L155 (2003).
[19] I. Opahle and P.M. Oppeneer, Phys. Rev. Lett. **90**, 157001 (2003).
[20] T. Maehira *et al.*, Phys. Rev. Lett. **90**, 207007 (2003).
[21] T. Gouder *et al.*, Phys. Rev. Lett. **84**, 3378 (2000).
[22] A.J. Arko *et al.*, *Handbook on the Physics and Chemistry of Rare Earths* (Elsevier Science, Amsterdam, (1999), Vol. 26, Chaps. 172, 265.
[23] J. J. Yeh and I. Lindau, At. Data Nucl. Data Tables **32**, 1 (1985).